Particle-in-cell simulations for Nanoplasmonic Laser Induced Fusion Experiments

István Papp, Larissa Bravina, Mária Csete, Archana Kumari, Igor N. Mishustin, Dénes Molnár, Anton Motornenko, Péter Rácz, Leonid M. Satarov, Horst Stöcker, Daniel D. Strottman , András Szenes, Dávid Vass, Tamás S. Biró, László P. Csernai, Norbert Kroó
(part of NAPLIFE Collaboration)

FIAS Frankfurt Institute for Advanced Studies

Nanoplasmonic Laser Inertial Fusion Experiment

Kőszeg, September 14, 2019 - Int. Workshop on Collectivity
First meeting on the NAPLIFE project (12 people)

Nanoplasmonic Laser Inertial Fusion Experiment

Conventional Thermonuclear Fusion

- Fusion does not happen spontaneously on Earth
- Total fusion energy $E_f = \frac{1}{4} n^2 \tau \epsilon \langle v\sigma \rangle$
- ηE_f is the usable energy
- The loss is $(1-\eta)(E_0 + E_b)$
- $E_0 = 3nkT$, $E_b = bn^2\tau\sqrt{T}$ (thermal bremsstralung)
- Giving the gain factor: $Q = \frac{\eta \epsilon n \tau v \sigma}{4(1-\eta)(3kT + bn\tau\sqrt{T})}$
- Q must be $Q > 1$ for energy production
- This also means $n\tau > \frac{3kT(1-\eta)}{\frac{1}{4}\epsilon\eta\langle v\sigma\rangle - b(1-\eta)\sqrt{T}} \rightarrow$ LC
- Fulfilling the Lawson criterion
  - Magnetically confined plasmas: increase confinement time
  - Inertial confinement fusion: increase density of fusion plasma

Direct vs Indirect drive

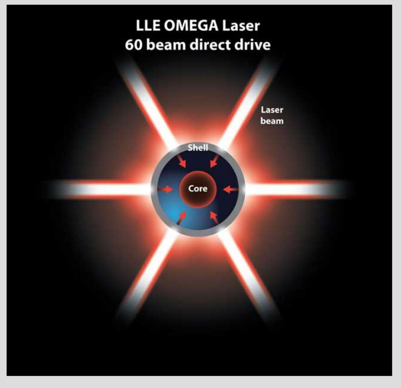

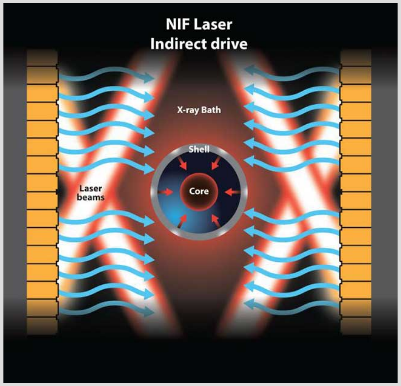

PHOTONICS MEDIA photonics.com

Rayleigh-Taylor instabilities

RFD

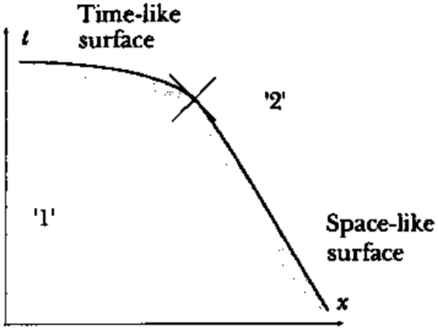

Figure 5.10: Smooth change from spacelike to timelike detonation

[Csernai, L.P. (1987). Detonation on a time-like front for relativistic systems. Zh. Eksp. Teor. Fiz. 92, 379-386.]

Constant absorptivity

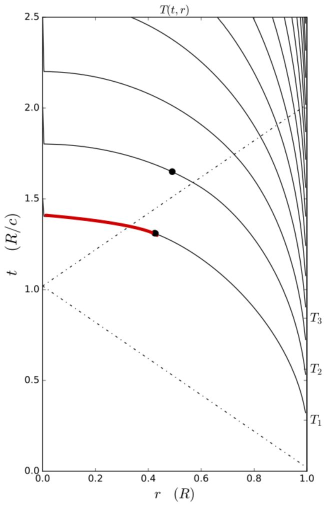

[L.P. Csernai & D.D. Strottman, Laser and Particle Beams 33, 279 (2015)]

$$\alpha_{k_{middle}} = \alpha_{k_{edge}}$$

Simultaneous volume ignition is only up to 12%

Nanoplasmonic Laser Fusion Research Laboratory

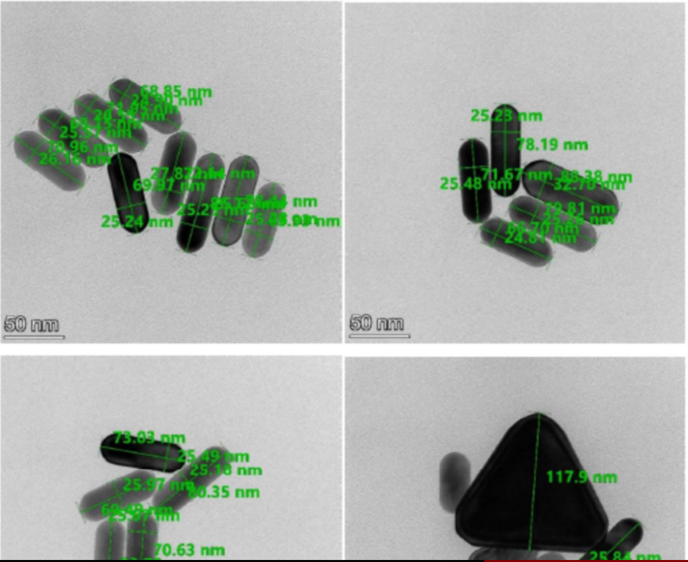

Transmission Electron-microscopy photos of 75x25 nm gold nano-rod antennas

[Judit Kámán, A. Bonyár et al. (NAPLIFE Collab.)., Gold nanorods …, 10th ICNFP 2021, **Kolymbari]**

Changing absorptivity

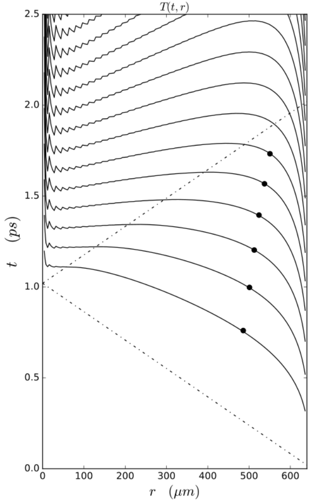

[Csernai, L.P., Kroo, N. and Papp, I. (2017). Procedure to improve the stability and efficiency of laser-fusion by nano-plasmonics method. Patent P1700278/3 of the Hungarian Intellectual Property Office.]

$\alpha_{k_{middle}} \approx 4 \times \alpha_{k_{edge}}$

Simultaneous volume ignition is up to 73%

Flat target

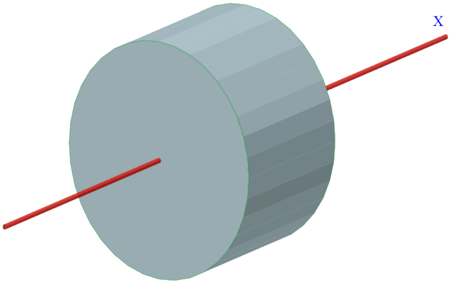

Schematic view of the cylindrical, flat target of radius, R, and thickness, h.
$V = 2\pi R^3$, $R = \sqrt[3]{V/(2\pi)}$, $h = \sqrt[3]{4V/\pi}$.

[L.P. Csernai, M. Csete, I.N. Mishustin, A. Motornenko, I. Papp, L.M. Satarov, H. Stöcker & N. Kroó, Radiation- Dominated Implosion with Flat Target, *Physics and Wave Phenomena*, **28** (3) 187-199 (2020)]

Varying absorptivity

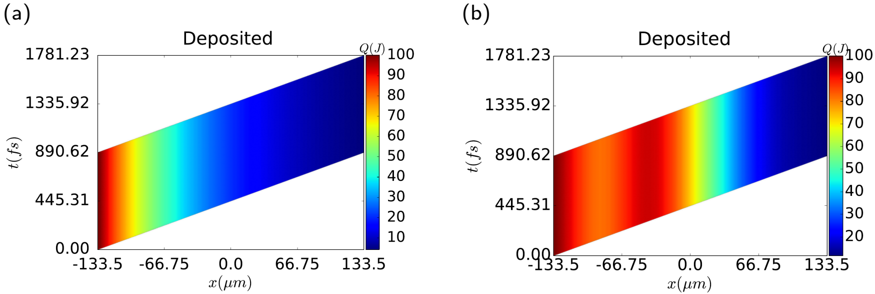

Deposited energy per unit time in the space-time plane across the depth, *h*, of the flat target. **(a) without** nano-shells **(b) with** nano-shells

To increase central absorption we used the following distribution:

$$\alpha_{ns}(s) = \alpha_{ns}^{C} + \alpha_{ns}(0) \cdot \exp\left[\frac{4x^2}{L^2 - x^2}\right] .$$

Particle In Cell methods

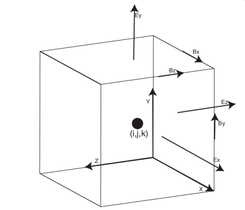

Figure 1. Yee staggered grid used for the Maxwell solver in *EPOCH*.

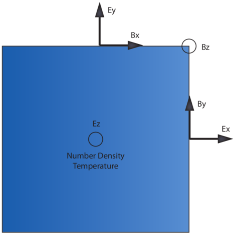

Figure 2: The Yee grid in 2D

[F.H. Harlow (1955). A Machine Calculation Method for Hydrodynamic Problems. Los Alamos Scientific Laboratory report LAMS-1956]

[T.D. Arber et al 2015 Plasma Phys. Control. Fusion 57 113001]

A **super-particle** (**marker-particle**) is a computational particle that represents many real particles.

Particle **mover** or **pusher** algorithm as standard **Boris algorithm**.

Finite-difference time-domain method for solving the time evolution of **Maxwell's equations**.

FDTD in EPOCH

- $\boldsymbol{E}_{n+\frac{1}{2}} = \boldsymbol{E}_n + \frac{\Delta t}{2}\left(c^2\nabla \times \boldsymbol{B}_n - \frac{\boldsymbol{j}_n}{\epsilon_0}\right)$
- $\boldsymbol{B}_{n+\frac{1}{2}} = \boldsymbol{B}_n - \frac{\Delta t}{2}\left(\nabla \times \boldsymbol{E}_{n+\frac{1}{2}}\right)$
- Call particle pusher which calculates j_{n+1}
- $\boldsymbol{B}_{n+1} = \boldsymbol{B}_{n+\frac{1}{2}} - \frac{\Delta t}{2}\left(\nabla \times \boldsymbol{E}_{n+\frac{1}{2}}\right)$
- $\boldsymbol{E}_{n+1} = \boldsymbol{E}_{n+\frac{1}{2}} + \frac{\Delta t}{2}\left(c^2\nabla \times \boldsymbol{B}_{n+1} - \frac{\boldsymbol{j}_{n+1}}{\epsilon_0}\right)$

Particle pusher

- Solves the relativistic equation of motion under the Lorentz force for each marker-particle

$$\boldsymbol{p}_{n+1} = \boldsymbol{p}_n + q\Delta t \left[\boldsymbol{E}_{n+\frac{1}{2}}\left(\boldsymbol{x}_{n+\frac{1}{2}}\right) + \boldsymbol{v}_{n+\frac{1}{2}} \times \boldsymbol{B}_{n+\frac{1}{2}}\left(\boldsymbol{x}_{n+\frac{1}{2}}\right)\right]$$

  $\boldsymbol{p}$ is the particle momentum q is the particle's charge $\boldsymbol{v}$ is the velocity.
  $\boldsymbol{p} = \gamma m \boldsymbol{v}$, where m is the rest mass $\gamma = \left[(\boldsymbol{p}/mc)^2 + 1\right]^{1/2}$

- Villasenor and Buneman current deposition scheme [Villasenor J & Buneman O 1992 Comput. Phys. Commun. 69 306], always satisfied: $\nabla \cdot \boldsymbol{E} = \rho/\epsilon_0$, where ρ is the charge density.

Particle shape

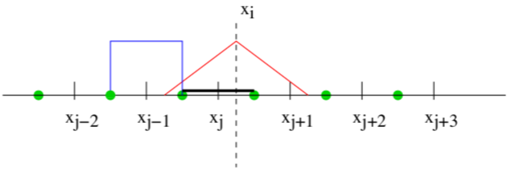

Figure 3: Second order particle shape function

First order approximations are considered

$$F_{part} = \frac{1}{2}F_{i-1}\left(\frac{1}{2} + \frac{x_i - X}{\Delta x}\right)^2 + \frac{1}{2}F_i\left(\frac{3}{4} - \frac{(x_i - X)^2}{\Delta x^2}\right)^2 + \frac{1}{2}F_{i+1}\left(\frac{1}{2} + \frac{x_i - X}{\Delta x}\right)^2$$

[EPOCH 4.0 dev manual]

Nanorod

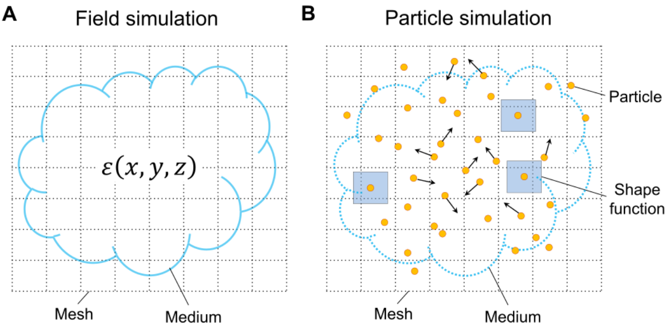

[W. J. Ding,et al., Particle simulation of plasmons Nanophotonics, vol. 9, no. 10, pp. 3303-3313 (2020)]

Nanorod

Typical Field solver:

$\epsilon(\omega) = 1 - \frac{\omega_p^2}{(\omega^2 + i\gamma\omega)}$

where ω_p is the plasma frequency: $\sqrt{\frac{n_e e^2}{m' \epsilon_0}}$

γ is the damping factor or collision frequency: $\gamma = \frac{1}{\tau}$ and τ is the average time between collisions

Particle simulation:

$$\frac{\partial \boldsymbol{E}}{\partial t} = \frac{1}{\mu_0 \epsilon_0} \nabla \times \boldsymbol{B} - \frac{\boldsymbol{J}}{\epsilon_0}, \; \frac{\partial \boldsymbol{B}}{\partial t} = -\nabla \times \boldsymbol{E}$$

$\gamma_i m_i \boldsymbol{v}_i = q_i(\boldsymbol{E}_i + \boldsymbol{v}_i \times \boldsymbol{B}_i)$, γ_i is the relativistic factor

Metal Nanoparticles as Plasmas

The conduction band electrons in metals behave as strongly coupled plasmas.
For golden nanorods of 25nm diameter in vacuum this gives an effective wavelength of $\lambda_{eff} = 266\text{nm}$

$$\frac{\lambda_{eff}}{2R\pi} = 13.74 - 0.12[\varepsilon_\infty + 141.04] - \frac{2}{\pi} + \frac{\lambda}{\lambda_p} 0.12\sqrt{\varepsilon_\infty + 141.04}$$

[Lukas Novotny, Effective Wavelength Scaling for Optical Antennas, Phys. Rev. Lett. **98**, 266802 (2007).]

Kinetic Modelling of the Nanorod

Nanorod inside a PIC simulation box in vacuum

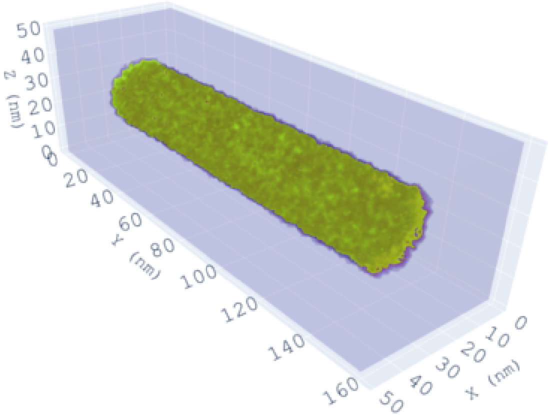

Kinetic Modelling of the Nanorod

Nanorod inside a PIC simulation box in UDMA

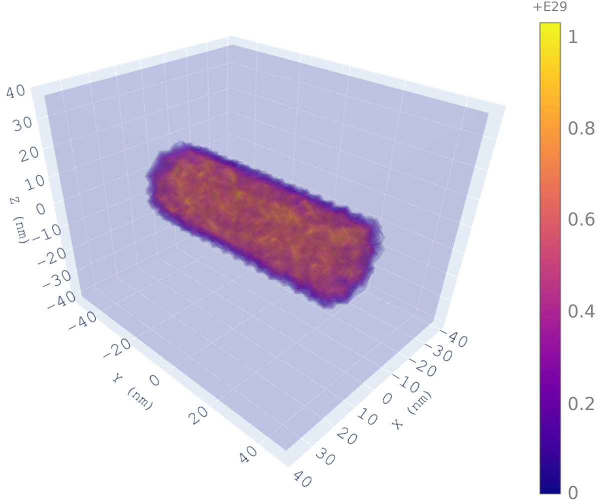

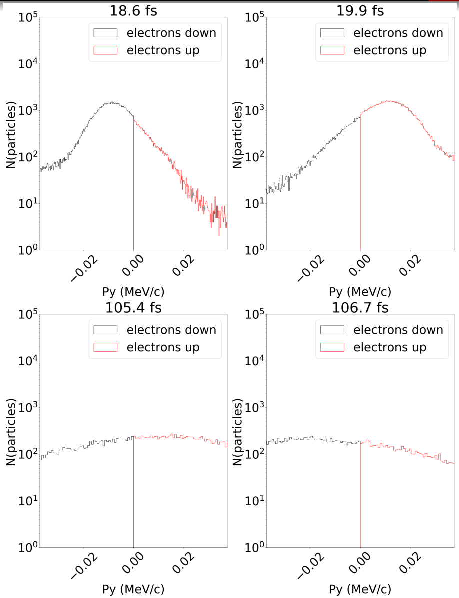

Considerations for the simulation box: $S_{CB} = 530 \times 530\text{nm}^2 = 2.81 \times 10^{-9}\text{cm}^2$ and length of $L_{CB} = 795\text{nm}$

beam crosses the box in $T = 795\text{nm}/c = 2.65\text{fs}$

Nanorod size: **25 nm** diameter with **130 nm length**

Pulse length: $40\times\lambda/c = 106$ fs
Intensity: 4×10^{15} W/cm^2

Kinetic Modelling of the Nanorod

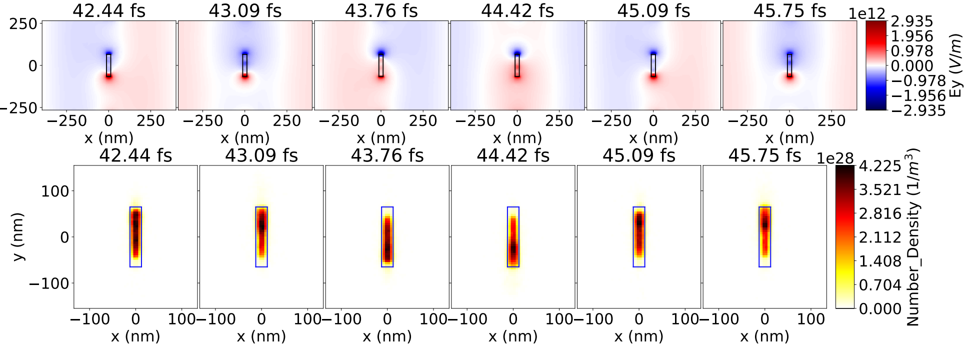

- Evolution of the E field's y component from 42.4 till 45.7 fs, around a nanorod of 25x130 nm.
- The direction of the E field at the two ends of the nanorod does not change.

Kinetic Modelling of the Nanorod

Evolution of the nanoantenna

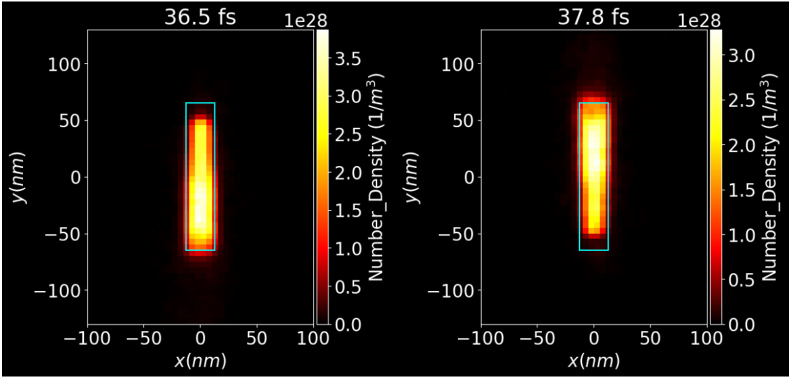

Number density of electrons in the middle of a nanorod of size 25x130 nm at different times. The nanorod is orthogonal to the beam direction, x.

In vacuum

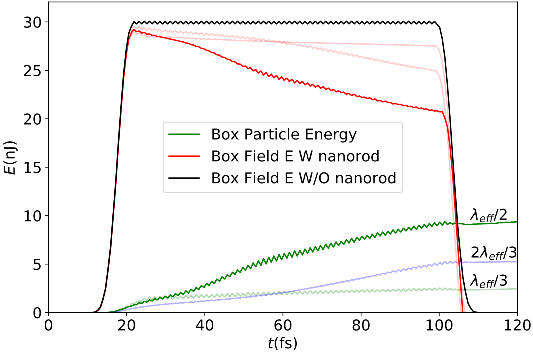

energy in the box **without nanorod** antenna 3×10^{-8} J (black line)
nanorod absorbs EM energy reducing it to 2.3×10^{-8} J (red line)
deposited energy in the nanorod (green line)
results in light absorption cross section highest

Comparison with other methods (Csernai, Csete et al.)

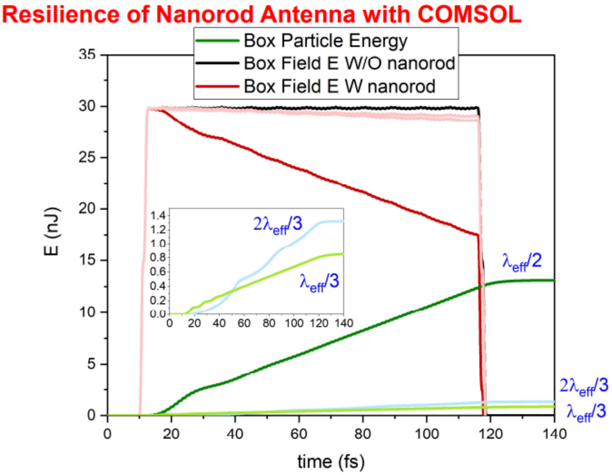

FEM computations with the same model parameters

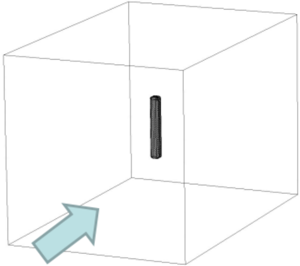

Good qualitative agreement between FEM and EPOCH/PIC methods
Quantitative difference:

In UDMA

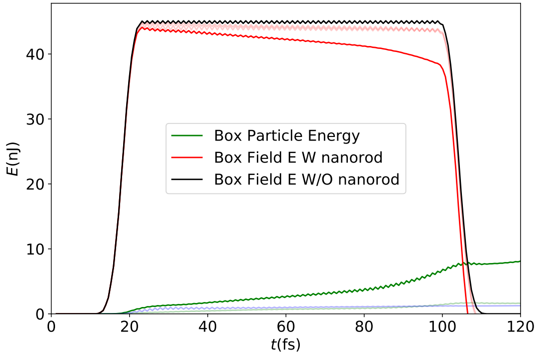

deposited energy in the nanorod (green line)

In UDMA and vacuum

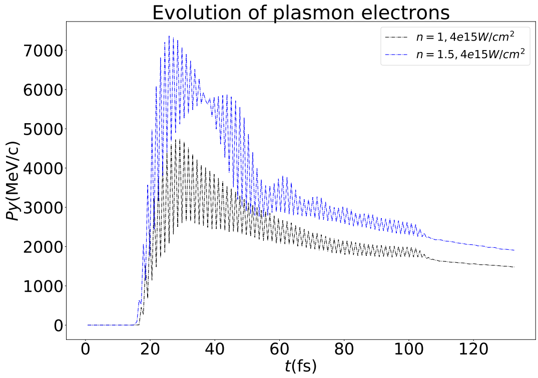

accumulated momentum of conduction electrons in **vacuum** (blue) and in **UDMA** (black) with their corresponding resonant length

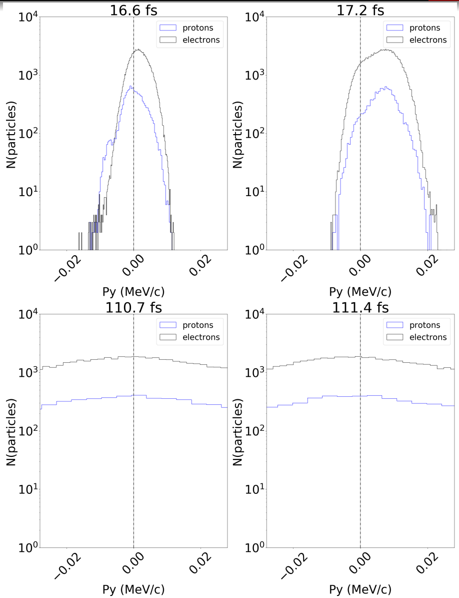

Protons surrounding the nanorod

Considerations for the simulation box:
$S_{CB} = 530 \times 530\text{nm}^2 = 2.81 \times 10^{-9}\text{cm}^2$ and length of $L_{CB} = 795\text{nm}$

beam crosses the box in $T = 795\text{nm}/c = 2.65\text{fs}$

Nanorod size: **25** nm diameter with **85 nm length**

Pulse length: $40 \times \lambda/c = 106$ fs
Intensity: 4×10^{15} W/cm^2

Conclusion and Outlook

- Our results agree with the those of Mária Csete in vacuum
- Quantitative differences mainly come at different lengths from resonance
- Levitation effect comes only in vacuum, needs further investigation
- Next step is estimating the target pre-compression